Chapter 3: One-dimensional boundary-value problems in electrostatics (15 Sep 2021)

A. One-dimensional configurations: general comments. (1)

B. Parallel-plate capacitor. (3)

C. Dipole layers. (4)

D. Depletion region of a semiconductor: approximate treatment. (6)

E. Piezoelectricity. (9)

F. Thomas-Fermi screening depth of a metal. (11)

G. Space-charge region of a semiconductor at finite temperatures. (13)

H. Forces on conductors via energy considerations. (14)

I. Forces on conductors: direct calculations. (17)

J. Green functions in one dimension. (18)

K. Green's First Identity and Green's Theorem in one dimension. (20)

L. Parallel-plate capacitor via Green's Theorem. (24)

A. One-dimensional configurations: general comments.

Not all of E&M is based on impenetrable equations. One-dimensional electrostatics is a case in point. Many important physical phenomena can be approximated accurately in this limit, for example screening in metals, space-charge regions of semiconductors, the CCD detector in the camera of your cell phone, double layers in electrochemistry, and work functions in electron emission, among many others. While geometries such as the parallel-plate capacitor obviously fall in the one-dimensional category, more general shapes also can be treated if the interface regions can be assumed to be locally flat, that is, if the local radius of curvature is large compared to the thickness of the interface or lateral extent of the region of interest. For example, in Ch. 1 we use the locally flat approximation to obtain the continuity conditions on normal and tangential components of electric and magnetic fields at the boundary between two media, taking the limit that the three dimensions of the "Gaussian pillbox" (Gauss' Theorem) and integration loop (Stokes' Theorem) are zero.

Additional reasons for studying one-dimensional configurations are that the material on Green functions, Green's Identities, boundary conditions, and methods of obtaining general theorems of electrostatics can be understood more easily in the more familiar mathematics of one dimension than three. This is done in the last three sections, which can be viewed as an introduction to Ch. 4.

For charge densities $\rho(\vec{r}) = \rho(z)$ that are one-dimensional functions of position and dielectric functions that are scalar, the fundamental electrostatics equations reduce to two:

$$\nabla \cdot \vec{D} = \frac{dD(z)}{dz} = 4\pi\rho(z); \tag{3.1a}$$

$$\vec{E}(z) = -\nabla\phi(z) = -\hat{z}\frac{d\phi}{dz}. \tag{3.1b}$$

These combine to yield Poisson's Equation

$$\frac{d^2\phi}{dz^2} = -\frac{4\pi\rho}{\varepsilon}. \tag{3.2}$$

The vector notation can be dropped for scalar ε because everything points in the $+\hat{z}$ or $-\hat{z}$ directions according to the sign of the results. E and ϕ are obtained by successive integrations:

$$\int_{z_o}^{z} dz' \frac{dE(z')}{dz'} = E(z) - E(z_o) = \frac{4\pi}{\varepsilon}\int_{z_o}^{z} dz'\,\rho(z'); \tag{3.3a}$$

$$\int_{z_o}^{z} dz' \frac{d\phi(z')}{dz'} = \phi(z) - \phi(z_o) = -\int_{z_o}^{z} dz'\left(E(z') - E(z_o)\right) \tag{3.3b}$$

Completing the transition from three dimensions to one dimension, the one-dimensional analog of the three-dimensional point charge q is the surface charge density σ, or

$$q\delta(\vec{r} - \vec{r}') \to \sigma\delta(z - z'). \tag{3.4}$$

The other situation, $\rho = \rho(\phi)$, can also be solved, although the path is indirect. We proceed as follows. Start by introducing z by writing

$$\int_{\phi_o}^{\phi} d\phi\rho(\phi) = \int_{z_0}^{z} dz' \frac{d\phi}{dz'}\rho(\phi). \tag{3.5}$$

Now

$$\frac{d^2\phi}{dz^2} = -\frac{4\pi\rho}{\varepsilon}, \tag{3.6}$$

hence

$$\int_{\phi_o}^{\phi} d\phi\rho(\phi) = -\frac{\varepsilon}{4\pi}\int_{z_0}^{z} dz' \frac{d\phi}{dz'}\frac{d^2\phi}{dz^2}. \tag{3.7}$$

But

$$\frac{d}{dz}\left(\left(\frac{d\phi}{dz}\right)^2\right) = 2\frac{d\phi}{dz}\frac{d^2\phi}{dz^2}$$

$$= \frac{d}{dz}\left(\vec{E}_z^{\,2}\right). \tag{3.8}$$

Therefore

$$\int_{\phi_o}^{\phi} d\phi\rho(\phi) = -\frac{\varepsilon}{8\pi}\int_{z_0}^{z} dz' \frac{d}{dz'}\left(\vec{E}^2(z)\right)$$

$$= -\frac{\varepsilon}{8\pi}\left(\vec{E}^2(z) - \vec{E}^2(z_o)\right). \tag{3.9}$$

Having $E^2(z)$, a square root followed by a second integration yields $\phi(z)$. This solution is of interest because in approximate form it describes Thomas-Fermi screening, done in Sec. F, and more generally, the accurate treatment of space-charge regions of semiconductors, done in Sec. G.

Thus in one dimension, "pulling the physics out of the math" essentially reduces to defining and interpreting accurate models. The best way to gain familiarity with how this objective is accomplished is by example. In the next section we give the humble parallel-plate capacitor significant attention not only as an example of solving Eqs. (3.2), but also as an example of superposition. In calculating forces on conductors, the superposition-based calculation introduces a perspective that will prove to be particularly useful in solving boundary-condition problems in later chapters. The Green-function solution in Secs. J and K anticipates the formal 3-dimensional approach of Ch. 4 in a simpler context, one where the Green function can be written down by inspection.

B. Parallel-plate capacitor: formal solution for fields and potentials.

The configuration is shown in the diagram. The plate at $z = 0$ is at $\phi = 0$, while the plate at $z = d$ is at $\phi = V$. The boundary conditions are $E = 0$ for $z \le 0$ and $z > d$, and $\phi = 0$ for $z \le 0$. For simplicity we assume that the dielectric is air, $\varepsilon = 1$, and that the plates are large enough relative to *d* so edge effects can be ignored. The objective is to determine $\phi(z)$ and the charge densities σ_1 and σ_2 on the plates by formally solving Eqs. (3.1). "Solution of Eqs. (3.1)" primarily reduces to finding and interpreting the relations connecting the different parameters d, V, σ_1, and σ_2 that describe the system.

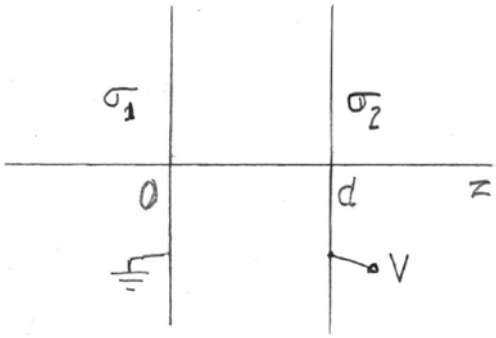

There are two ways to proceed: informally through diagrams, or formally starting with

$$\rho(z) = \sigma_1\delta(z) + \sigma_2\delta(z-d). \tag{3.10}$$

Doing the formal solution first, direct integrations yield

$$E(z) = 4\pi\sigma_1 u(z) + 4\pi\sigma_2 u(z-d); \tag{3.11a}$$

$$\phi(z) = -4\pi\sigma_1 z u(z) - 4\pi\sigma_2 (z-d)u(z-d); \tag{3.11b}$$

where $u(z)$ is the Heaviside or unit-step function equal to zero or one if the argument is negative or positive, respectively. E is automatically zero for $z \le 0$, and is zero for $z > d$ if $\sigma_1 + \sigma_2 = 0$. With $\phi = V$ at $z = d$, $-\sigma_1 = \sigma_2 = \dfrac{V}{4\pi d}$, so the full solution is

$$-\sigma_1 = \sigma_2 = \frac{V}{4\pi d}. \tag{3.12}$$

The solution is shown in the figure at the right. The informal approach starts with the diagram of $\rho(z)$, then follows with successive integrations to determine E and ϕ without formally writing $\rho(z)$ explicitly. This works here because the configuration is simple enough to be solved by inspection. Nevertheless, the formal solution has the advantages that

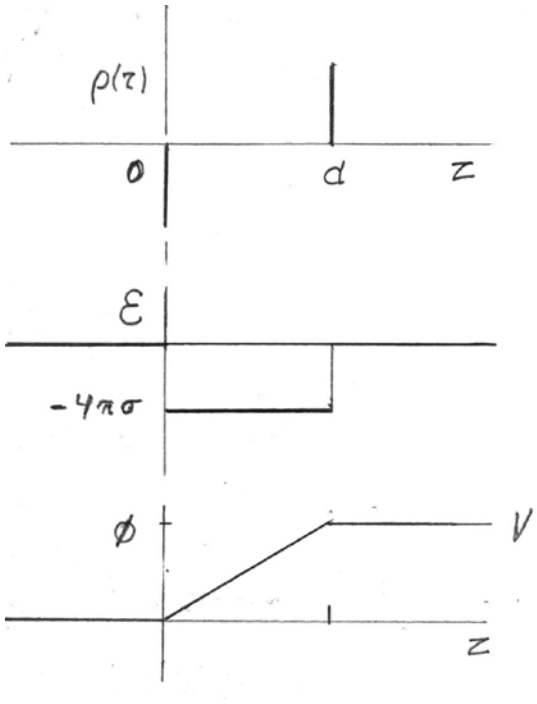

(1) $\rho(z)$ is self-contained. No additional defining statements or constraining conditions are required.

(2) The boundary conditions enter naturally in the integrations.

(3) The expressions for $E(z)$ and $\phi(z)$ are also self-contained, requiring no additional statements or constraints.

(4) The original problem is reduced to crank-turning, which will prove to be useful in more complicated geometries.

Repeating the comment above, even with the formal solution, a diagram reduces opportunities for errors by making it easier to keep track of what is going on.

We will return to the capacitor in Secs. H and I. The objective there is to calculate the pressure on the plates, which is done from several perspectives to compare how different kinds of physics can be used to achieve this goal.

C. Dipole layers.

These are atomic-scale versions of the parallel-plate capacitor. Dipole layers are common in chemistry and physics, and can be thought of as capacitors in the limit where $d \to 0$ but where $\Delta V = 4\pi\sigma d$ remains finite. The result is a jump ΔV in potential as the double-layer is crossed. Jackson discusses double layers in Sec. 1.6 using a three-dimensional approach, which while correct is considerably more complicated than necessary. Two physical examples of double layers follow.

(1) Electrochemical double layers.

In principle, ionic double layers form whenever a solid is immersed in a fluid containing ions. Either positive or negative ions collect at the interface, resulting in a discontinuity in the field on the nm scale. If the solid is a metal, then the resulting field is screened over the order of 0.1 nm in the metal by an induced charge of opposite sign, as calculated in Sec. F. Double layers are a feature of any heterogeneous solution

containing a stable suspension of particles, for example milk, paint, blood, etc. The particles themselves adsorb ions from solution, leading to repulsive interparticle interactions that prevent aggregation and settling out.

A one-dimensional example is an electrochemical cell consisting of an Au electrode in an aqueous KCl solution. At an appropriate potential Cl^- ions adsorb on the Au surface, driving some of the mobile electrons of the metal away from the surface region and exposing a fraction of the positive atomic cores, as shown in the diagram. A detailed treatment requires the use of quantum mechanics, which would also take into account the lateral inhomogeneities of the potential.

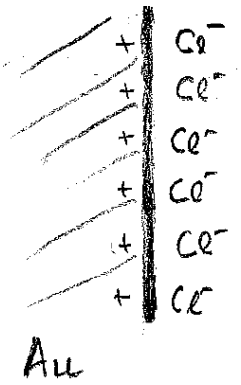

However, we can idealize the configuration by averaging over lateral dimensions, thereby turning the partially exposed metal atoms into a sheet of uniform surface charge density $+\sigma$ at $z = -d$, and replacing the Cl^- ions by a similar sheet of uniform surface charge density $-\sigma$ at $z = 0$. The result is a reasonable approximation to the physical situation observed on the laboratory scale. The net result is a high-field region between the two layers of charge, and an overall change of the potential by an amount $\Delta V = -4\pi\sigma d$ from the bulk of the metal to the electrolyte. We are left with a configuration that is identical to that of the parallel-plate capacitor.

(2) Work functions.

The work function is the energy required to extract an electron from a material, usually a metal. Work functions necessarily involve interfaces, commonly between a metal and the vacuum. When vacuum tubes were current technology, considerable effort was invested in reducing cathode work functions so electrons could be emitted at the lowest possible filament temperatures. This was done for sound economic reasons: the high temperatures required for useful emission meant that filaments were voracious consumers of power. In addition, they burned out regularly. Attempts to improve emission included coating cathodes with easily ionized materials such as Cs. The Cs atoms donate electrons to the cathode, and the ionized Cs atoms function as an effective positive sheet of charge about one atomic distance away from the metal surface. Cs coating reduced barriers for electron emission from about 5 eV to about 2 eV. Unfortunately, metals such as Cs also oxidize easily, so commercial cathodes were fabricated using less reactive materials. However, Cs-coated surfaces remained useful in the early days of photoemission experiments.

Recognizing that a more energy-efficient technology was needed to meet the increasing demands of telephone service, in the early 1940s AT&T management tasked Bell Telephone Laboratories to find replacements not only for vacuum tubes but also for mechanical switching relays, which were also notoriously unreliable. This goal-oriented research led directly to the invention of the Ge point-contact transistor in 1947. For this invention Bardeen, Brattain, and Shockley were awarded the Nobel Prize in Physics in 1956, over strenuous objections by establishment physicists for giving such prestigious recognition to “dirt physics” (T. D. Lee and C. N. Yang presumably had to wait another year to be recognized for parity violation.)

While work on negative-electron-affinity cathodes continued, its later objectives were to realize electron emission at room temperature. Among other efforts, this research was directed toward wide-bandgap semiconductors such as GaN or AlN, where the conduction band edges are already near or above the vacuum level, so that in principle an electron can lower its energy by escaping from the material.

Work functions on bare metal surfaces are interesting examples of double layers, because the electron wave functions of different facets of metal crystals terminate differently. This translates into different effective sheets of charge, and therefore different work functions. Taking Ir as an example, the work functions of clean surfaces in ultrahigh vacuum are as follows, by crystal facet:

Surface:	Work function:
(111)	5.76 eV
(100)	5.67
(110)	5.42
(210)	5.00

These data illustrate directly that surface dipole layers depend on orientation.

D. Depletion region of a semiconductor: approximate treatment.

Another example where charge density is a function of position is the space-charge region of a semiconductor. This is essentially a dielectric-filled capacitor whose plate separation depends on the applied potential V. From a basic-physics perspective the charge density in this configuration is actually a function of ϕ, as discussed in Sec. G, but in practice the present solution is a good approximation.

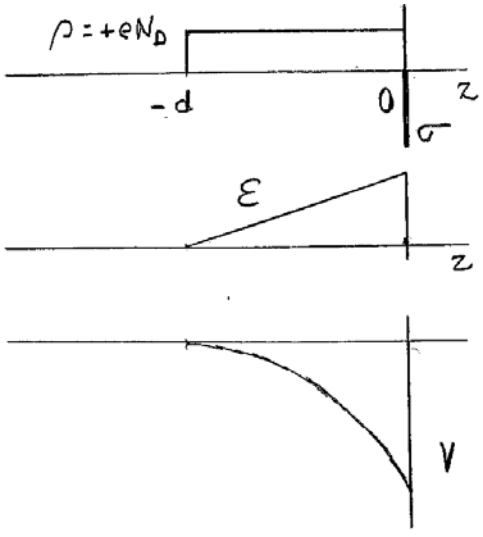

The schematic depicting the spatial dependences of the charge, field, and potential of an *n*-type semiconductor with the back side and interior at zero potential and the surface at a negative potential V is shown at the right. The semiconductor is doped with impurity atoms with a valence one greater than that of the replaced atom, for example P in Si or Se for As in GaAs. The electron leaves the impurity atom and resides as a carrier free to move in the conduction band. Such impurity concentrations are not large, typically only parts per million, but the fact that the resulting carrier concentrations can be controlled in various ways and modified by external fields yields huge technological dividends. If no surface voltage is applied, the extra electrons are compensated by the extra charge of the cores, so the system is neutral.

However, if a negative potential $\phi = -V$ is applied to the surface, the electrons are repelled from the surface region. Since the impurity atoms are fixed in the lattice and

cannot move, the surface region is left to a depth d with a net positive charge density e times the impurity concentration n_D. The situation is shown in the above diagram. The solution connects the parameters d, n_D, V, and the dielectric constant ε, given the boundary conditions $\phi(z) = 0$ and $E(z) = 0$ for large negative z, $\phi = -V$ at $z = 0$, and $E(z) = 0$ for $z > 0$. The approximation here is that the boundary at $z = -d$ is abrupt.

With a negative potential V applied to the contact, the charge density for $z > -d$ is formally

$$\rho(z) = en_D\left(u(z+d) - u(z)\right) + \sigma\,\delta(z), \tag{3.13}$$

where the first two terms describe the semiconductor and the third the metal contact. From the above discussion, we expect that $\sigma < 0$. Restating this in less intimidating terms, we have

$$\rho(z) = 0 \qquad \text{for } z < -d \text{ and } z > 0; \tag{3.14a}$$

$$= en_D \qquad \text{for } -d \le z < 0; \tag{3.14b}$$

$$= \sigma\delta(z) \qquad \text{for } z = 0, \tag{3.14c}$$

as indicated in the diagram.

Solution by successive integrations is the appropriate approach. Because the dielectric function of a semiconductor is of the order of 10 or greater, we retain ε. Then the first integral gives

$$D(z) = 0 \qquad \text{for } z \le -d; \tag{3.15a}$$

$$= 4\pi en_D(d+z) \qquad \text{for } -d \le z < 0; \tag{3.15b}$$

$$= 0 \qquad \text{for } z > 0; \tag{3.15c}$$

where $D(z) = \varepsilon E(z)$. The integration for ϕ yields

$$\phi(z) = 0 \qquad \text{for } z < -d; \tag{3.16a}$$

$$= -\frac{2\pi en_D}{\varepsilon}(d+z)^2 \quad \text{for } -d \le z < 0\ 0 \le z \le d; \tag{3.16b}$$

$$= -\frac{2\pi en_D}{\varepsilon}d^2 = V \quad \text{for } z \ge 0. \tag{3.16c}$$

Therefore

$$V = -\frac{2\pi en_D}{\varepsilon}d^2 < 0; \tag{3.17a}$$

$$d = \sqrt{-\varepsilon V/(2\pi en_D)}; \tag{3.17b}$$

noting that in Eq. (3.17b), $V < 0$. The charge Q per unit area A stored on the metal contact is

$$\frac{Q}{A} = \sigma = \frac{D(0)}{4\pi`} = -eN_D d = -\sqrt{\frac{-\varepsilon\, en_D V}{2\pi}}\,, \tag{3.18}$$

which is negative, as expected, and equals the charge removed from the space charge region. The capacitance per unit area is therefore

$$\frac{C}{A} = \frac{\sigma}{V} = \sqrt{\frac{\varepsilon e n_D}{2\pi |V|}}\,. \tag{3.19}$$

The *differential* capacitance, which is the value relevant to the operation of small-signal devices, is

$$\frac{C_d}{A} = \frac{d\sigma}{dV} = \frac{1}{2}\sqrt{\frac{\varepsilon\, en_D}{2\pi |V|}}\,. \tag{3.20}$$

This is half the static capacitance *C*. Thanks to the dependence of the back capacitor "plate" on V, both capacitances are functions of *V*. Making *V* more negative increases the length of the depletion region, thereby reducing the capacitance.

For completeness, the more accurate representation of the charge density in the semiconductor is

$$\rho = \rho(\phi) = en_D\left(1 - e^{e\varphi/kT}\right) - \sigma\,\delta(z)\,. \tag{3.21}$$

This expression, discussed in Sec. G, is based on the Boltzmann approximation, where the concentration of electrons in the conduction band is given locally by $n_D e^{e\varphi/kT}$, where $\phi = \phi(z)$ is electrostatic potential measured relative to a zero deep within the semiconductor. The general solution describes both depletion and accumulation regions at finite temperatures depending on whether ϕ is negative or positive, respectively. Not surprisingly, the mathematics behind Eq. (3.21) is considerably more complicated than that leading to Eqs. (3.17).

The depletion-mode approximation describes the operation of pixels in the charge-coupled-device (CCD) detector used in your cell-phone and other cameras. With current 48 Mpixel technology each pixel is 0.8 μm × 0.8 μm in area. During operation, each pixel is charged up to the same predetermined voltage V_0 (negative for an *n*-type semiconductor, as in the above calculation). The shutter is then opened, and photons are absorbed in proportion to the quantum efficiency of the device. Each absorbed photon generates an electron-hole pair. Following the absorption event, the electron joins the other electrons in the bulk of the material, and the hole migrates to the contact, reducing the number of electrons stored there by 1. Thus the pixel discharges according to integrated intensity. Because the number of stored electrons is finite, there is an upper limit to the number of photons that can be recorded before the depletion region collapses completely and the pixel saturates.

After the shutter is closed, the electronics monitors the charge necessary to reset the pixel to its original voltage $(-V_o)$ while monitoring the charge necessary to accomplish this. The charge map is then displayed in two dimensions, forming the picture. The

advantage of depletion-mode operation is that the signal read out of any given pixel does not depend on the detailed properties of the pixel, so some variations in properties, for example doping nonuniformities, are possible and the camera still returns faithful images.

George Smith and Willard Boyle of Bell Laboratories, the inventors of the CCD (charge-coupled-device) version of this technology, were awarded half the Nobel Prize in physics in 2009, the other half going to Charles Kao (Standard Telecommunications Laboratories) for his work on optical fibers.

E. Piezoelectricity.

Another physical phenomenon that can be described to a good approximation by one-dimensional electrostatics is piezoelectricity. Here, the application of a compressive stress to a properly oriented crystal generates potential differences that can be quite large. This effect is used for example for firing spark plugs in small engines of the type found on lawn mowers, chain saws, etc.

Although the material of choice for generating usefully high voltages is the perovskite lead zirconate titanate (PZT), the phenomenon and the physics behind piezoelectricity can best be understood by considering a crystal of GaAs cut with its surfaces perpendicular to the (111) direction, as shown at the top of the next page. Although GaAs is neither sufficiently polar nor sufficiently strong to be viable commercially as a piezoelectric material, it is a good example because its face-centered-cubic crystal structure is relatively simple and its parameters are accurately known.

Without getting into details of crystal orientations, the figure at the right shows a schematic of the material with the *z*-axis along the body diagonal of the unit-cell cube. From this perspective the As and Ga atoms lie in separate planes. For this tetrahedrally covalently bonded material, roughly speaking each As atom donates an electron to a Ga atom, so that the As and Ga planes can be idealized as adjacent sheets of alternating charge densities $+\sigma$ and $-\sigma$, respectively. Given its crystal structure and 0.565 nm lattice constant, the bond length (the larger spacing between planes) is 1/4 the body diagonal of the cube, or 0.245 nm. With the smaller spacing 1/3 of this, or 0.0816 nm, the projection pattern consists of slightly distorted hexagons. The repeat period *d* between planes of like charge is then 0.326 nm. Thus there are approximately 3.1×10^7 pairs of planes per cm of material.

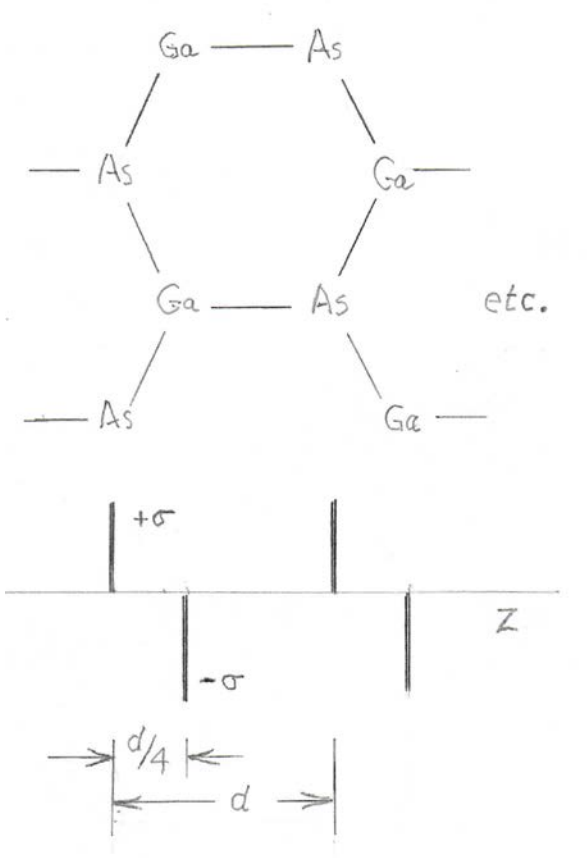

When the crystal is compressed along the *z* direction of the diagram above, the bond length remains approximately constant but the bonds along the zigzag directions tend to flatten. Thus the narrower spacing between planes becomes even narrower, while the larger spacing remain essentially constant. Although this model is almost a criminally oversimplified, it allow us to answer questions as to why an applied stress can generate large voltages across macroscopic samples, how large these voltages are likely to be, the effect of charge (typically H_3O^+ or HCO_3^-) adsorbed on the surfaces of the crystal, and why crystal structure is important. The equilibration time of this adsorbed charge is a factor in determining the voltages generated.

We solve the problem using the formal approach, defining the charge density, then integrating Gauss' Equation twice. The diagram on the next page illustrates the results. The charge density is

$$\rho(z) = \sigma \sum_{n=0}^{N} \big(\delta(z - nd) - \delta(z - d/4 - nd)\big). \tag{3.22}$$

The first integration yields the field

$$E(z) = \frac{D(z)}{\varepsilon} = \frac{4\pi\sigma}{\varepsilon} \sum_{n=0}^{N} \big(u(z - nd) - u(z - d/4 - nd)\big), \tag{3.23}$$

as shown in the middle part of the figure. The second integration yields the potential

$$\phi(z) = -\frac{4\pi\sigma}{\varepsilon} \sum_{n=0}^{N} \big((z - nd)u(z - nd) - (z - d/4 - nd)u(z - d/4 - nd)\big), \tag{3.24}$$

as shown at the bottom.

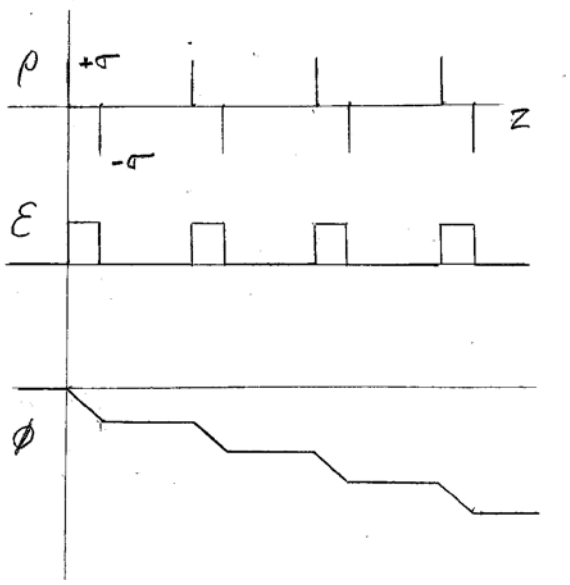

Thus *E* alternates between zero and $4\pi\sigma/\varepsilon$, while ϕ decreases by $\Delta\phi = \pi\sigma d/\varepsilon$ per cell as a result of the contribution from the pair of planes with narrower spacing. Given that the volume density of atoms in GaAs is 4.43×10^{22} cm^{-3}, the areal density of atoms in a given plane is 7.17×10^{14} cm^{-2}. Assuming that σ corresponds to 1 electron/atom, with a static dielectric constant of $\varepsilon = 12.9$, this field in SI units is $E = \sigma/\varepsilon\varepsilon_0 = 1.00\times10^8$ V/cm. Thus the contribution per cell is 0.82 V. With $N = 3.1\times10^7$ cells across a crystal of thickness 1 cm, this results in a voltage of about 26 megavolts, a respectable number indeed.

Yet if you should find such a crystal lying around on a table, these voltages are not observed. Why? First, our calculation is considerably oversimplified, and overestimates

the potential realized per unit cell. Second, and more important, the combination of oxidation and the fact that air contains both positive and negative ions, for example HCO_3^- and H_3O^+, results in the formation of sheets of physi- or chemisorbed charge on the surface that counteracts the voltages that would otherwise be generated. We can calculate the charge density of these adsorbed layers by requiring that these large potentials are cancelled. Adsorbing a layer of surface-charge density $\sigma_A = -\sigma/4$ to the layer at $z = 0$ and a layer of opposite surface-charge density to the last layer is seen by linear superposition to generate a potential that cancels the monatomic increase, leading to a net potential increase of zero per cell, and hence zero overall. These adsorbed surface-charge layers are extremely important in practice, as is well known in the xerography industry.

We now suppose that the material is compressed by an amount Δd per unit cell, that all the compression occurs at the narrower spacing, and that this is done quickly enough so the amount of charge physi- or chemisorbed on the surfaces does not change. Given that the net electric field in this region is

$$E = 4\pi\sigma(1-1/4) = 3\pi\sigma\,, \tag{3.25}$$

we obtain a change $\Delta\phi$ of ϕ across each unit cell to be

$$\Delta\phi = 3\pi\sigma\,\Delta d\,. \tag{3.26}$$

With the above values, at the strain limit of 0.5% for GaAs, piezoelectricity can generate about 12.2 mV per cell, or about 380 kV across 1 cm of material. This is obviously more than enough to fire a spark plug.

The calculation also shows that if the compression had been distributed equally between planes, as would be the case if GaAs were compressed in the (001) direction (parallel to the edges of the cube), then the rise and fall of potential between planes would cancel. No net voltage would be generated. Random orientation of bonds, as occurs with amorphous material, yields the same result. Thus in piezoelectricity, crystal symmetry is all-important.

Interface charges also present a complication in the heteroepitaxial growth of polar materials on nonpolar surfaces, for example the growth of GaAs on Si. However, these effects can also be used to engineer high internal electric fields to enhance device operation by accelerating free carriers. All these phenomena can be understood qualitatively using the simple one-dimensional model discussed above.

F. Thomas-Fermi screening depth of a metal.

We now consider configurations where $\rho = \rho(\phi)$. The standard example is Thomas-Fermi screening. When an electric field $\vec{E}$ is applied to a metal surface, a screening charge σ is developed that we usually idealize as a layer of zero thickness. However, as mentioned in the previous chapter, this idealization is not quite accurate. This field penetrates a finite depth into the metal, decaying approximately exponentially as shown schematically in the diagram at the top of the next page.

The calculation differs from that of the depletion mode in semiconductors discussed above because the density of free electrons n_c in the conduction band of a metal greatly exceeds that which is possible to attain in a doped semiconductor. Hence complete depletion is never achieved. For example, the electron density in Au is 5.77×10^{22} cm^{-3}, which is about two orders of magnitude beyond anything that can be achieved in a doped semiconductor. As a result, the decay length of the charge density, called the Thomas-Fermi screening length, is much shorter than is the case in semiconductors, being only of the order of one atomic separation.

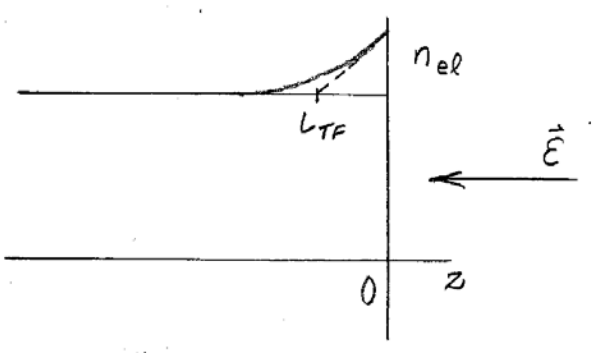

To perform the calculation, we approximate the local change in electron density as a Boltzmann distribution

$$\Delta n = \Delta n_c \cong n_c(e^{e\phi/kT} - 1). \tag{3.27}$$

Although electrons obey Fermi-Dirac statistics, Eq. (3.27) is a reasonable approximation to the ϕ dependence because the states at the Fermi level itself are only half filled. Here, n_c is the density of electrons in the material, and ϕ is measured from the Fermi level ϕ_F, which is usually of the order of several eV above the bottom of the conduction band. The sign of ϕ is consistent with expectations: Δn is positive for positive potentials.

Starting from Poisson's Equation, we seek to estimate the effective depth to which the normal component of an external field $\vec{E}$ penetrates the metal. The problem is solved approximately by assuming that $\varepsilon = 1$, which is usually a good approximation for metals since the dominant contribution to ε arises from free charge, not the lattice. Also, if we assume that the maximum value of ϕ is small compared to *kT*, the exponential in Eq. (3.27) can be expanded. Then

$$\frac{d^2\phi}{dz^2} = -4\pi\sigma(\phi) \approx 4\pi e n_c \frac{e\phi}{kT}. \tag{3.28}$$

To solve Eq. (3.28), assume that ϕ has the form $\phi = \phi_0 e^{z/L_{TF}}$, where L_{TF} is the Thomas-Fermi screening length. Making the substitution we find

$$L_{TF}^2 = \frac{kT}{4\pi e^2 n_c}. \tag{3.29}$$

Inserting the room-temperature value $kT = 0.025$ eV and noting that $e^2/(2a_B) = 1$ Rydberg = 13.6 eV, where $a_B = 0.529\times10^{-10} m$, we obtain $L_{TF} = 0.12$ nm. Therefore, field penetration depths are indeed of the order of atomic separations.

We still need to verify that ϕ is small enough for the first-order approximation to be valid. Since $\phi(z) = \phi_0 e^{z/L_{TF}}$ we have at the surface

$$E(z) = -\frac{d\phi}{dz} = -\frac{\phi_0}{L_{TF}} e^{z/L_{TF}} \quad E(0) = -\left.\frac{d\phi}{dz}\right|_{z=0} = \frac{\phi_o}{L_{TF}}. \tag{3.30}$$

Given the atomic-scale magnitude of L_{TF}, very large surface fields can be obtained with very small potentials. For example, a field $E = 10^6$ V/cm, which is essentially the limit that can be realized in electrostatics, yields

$$\phi_0 = (10^6\ V/cm)(10^{-8}\ cm) = 0.01 V\,. \tag{3.31}$$

This is sufficiently smaller than the room temperature value of *kT* to suggest that the first-order treatment is at least reasonable. Finally, the local charge density $\rho(z)$ is given by

$$4\pi\,\rho(z) = -\frac{d^2\phi}{dz^2} = -\frac{\phi_0}{L_{TF}^2} e^{z/L_{TF}}\,. \tag{3.32}$$

Integrating this from $z = -\infty$ to the surface $z = 0$ yields

$$4\pi\,\sigma = 4\pi \int_{-\infty}^{0} \rho(z)dz = -\frac{\phi_0}{L_{TF}} = E\,, \tag{3.33}$$

which is the electrostatic result. Thus while the thickness of the screening-charge layer at the surface of a metal is not quite zero, it is close enough to zero for all practical purposes.

G. Space-charge region of a semiconductor at finite temperatures.

The space-charge region of a semiconductor is a second example of a configuration where ρ is a function of ϕ. From Eqs. (3.9) and (3.21) and the discussion in Sec. D, the charge density is

$$\rho(\phi) = eN_D\left(1 - e^{e\phi/kT}\right) + \delta(z)\,, \tag{3.34}$$

where ϕ is referenced to $\phi = 0$ deep within the semiconductor where the concentration of donors equals the concentration of electrons so the material is neutral. For typical doping levels, the occupancy of conduction-band states is so low that Boltzmann statistics is an excellent approximation. As the potential becomes more negative, the density of electrons, which is equal to $N_D e^{e\phi/kT}$, disappears and the positive donors dominate. Alternatively, as ϕ gets more positive, the electron contribution increases exponentially with ϕ, and the surface region goes into accumulation. Thus Eq. (3.32) covers both depletion and accumulation. Also, the combination $\left(1 - e^{e\phi/kT}\right)$ gives a more accurate assessment of the behavior of the charge density at the back of the space charge region than the primitive sharp cutoff that we used in Sec. D.

We evaluate the expression according to Eq. (3.9). Integration yields

$$\left(\frac{d\phi}{dz}\right)^2 = 8\pi kTN_D\left(e^x - x - 1\right), \tag{3.35}$$

where $x = e\phi/kT$. The right-hand side of Eq. (3.35) is obviously positive definite for large values of *x*, either positive or negative, consistent with expectations. By expanding the exponential for small *x*, it is seen to be positive there as well. Thus no sign problems are encountered in taking the square root of both sides. The expression to be evaluated to obtain ϕ as a function of *z* is therefore

$$\int_z^0 dz = -z = \int_\phi^V \frac{d\phi}{\sqrt{8\pi kTN_D(e^x - x - 1)}}\,. \tag{3.36}$$

The expression is logarithmically divergent for $\phi \to 0$, which is why we must reference both *z* and *V* to the surface at *z* = 0.

Equation (3.36) can be evaluated approximately in the limit that e^x is either so large that it dominates the remaining terms in the denominator (large positive *V*), or so small that it can be neglected (large negative *V*). These represent the accumulation- and depletion-mode limits, respectively, for an n-type semiconductor, and the situation for $T \to 0$. However, if the remaining terms in the argument of the square root are not taken into account as $\phi \to 0$, then the logarithmic divergence is lost. The depletion-mode situation for large negative *V* is more amenable to a closed-form treatment. By setting $\phi = 0$ we find that the depletion depth is

$$-z = d = \sqrt{\frac{-V}{2\pi N_D e}}\,, \tag{3.37}$$

in agreement with Eq. (3.17b). The temperature has dropped out of Eq. (3.37) completely, which is physically reasonable because it is assumed that all electrons are removed from the space charge region, and that the boundary to the neutral region is sharp.

H. Forces on conductors via energy considerations.

The calculation of the electrostatic force on a conductor in an electric field provides insight into some unexpected aspects of forces, energies, fields, and superposition. We discuss this in the present and following sections. There are several ways to do this. Our first approach uses energy balance, and considers a differential area ΔA on the surface of a conductor that is small enough so this region of the conductor can be considered locally flat. Assuming a field $\vec{E}(\vec{r})$ is applied to the conductor, Stokes' Theorem shows that $\vec{E}(\vec{r})$ must be normal to ΔA. Also, because there is no field inside the conductor, Gauss' Law shows that $\vec{E}$ induces a local surface charge density $\sigma = E/4\pi$ at ΔA. The energy density U_E adjacent to ΔA is therefore

$$U_E = \frac{1}{8\pi}\vec{E}^2 = 2\pi\sigma^2. \tag{3.38}$$

If σ remains constant, then to first order a displacement *dz* of ΔA that increases the volume also increases the stored energy. This increase is given by

$$d(\Delta W) = U_E \Delta A\, dz = (2\pi\sigma^2 dz)\,\Delta A$$

$$= (\Delta\vec{F} \cdot \hat{z})dz\,, \tag{3.39}$$

where $\Delta\vec{F}$ is the force needed to move the area element ΔA by *dz*. Since the conductor is in mechanical equilibrium, this force is balanced by the force $(-\Delta\vec{F})$ exerted by the field on the area ΔA of the plate. Conservation of energy requires that the energy stored in the system changes by the same amount as the mechanical work done to displace ΔA by *dz*. With σ constant we have

$$\frac{\Delta F}{\Delta A} = 2\pi\sigma^2\,. \tag{3.40}$$

Therefore, the force per unit area (pressure) is normal to the surface, has a magnitude $2\pi\sigma^2$, and is directed toward the region containing the field. This is the direction that we would expect, given that all systems seek to minimize their energies. We also see that pressure is simply equal to the energy density, which we already knew from thermodynamics. We emphasize that this calculation assumes that σ is a constant, independent of the displacement *dz*.

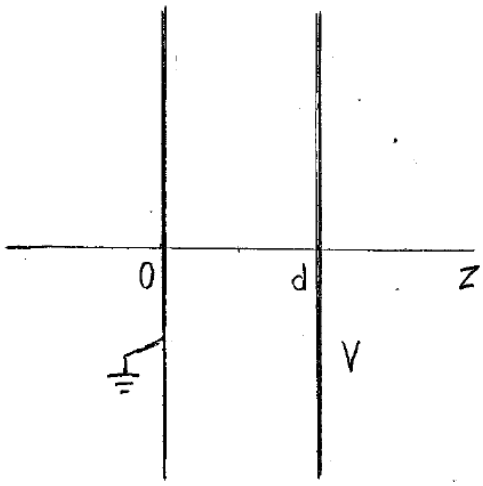

But if taken at face value, the above calculation is not quite as simple as it appears. We generate some apparent contradictions and obtain additional insights by considering the parallel-plate capacitor shown in the diagram. The plates are perpendicular to the *z* axis, with one plate intersecting the axis at *z* = 0 and the other at *z* = *d*. The plates are charged to a voltage difference $V = Ed$, with the potential of the plate being zero at $z = 0$. Thus the plates carry surface charge densities of $(-\sigma)$ and $(+\sigma)$, respectively, where $4\pi\sigma = E = V/d$. If the area *A* of the plates is large enough relative to d so edge effects can be ignored, then the total energy stored in the capacitor is

$$W = 2\pi\sigma^2 Ad\,. \tag{3.41}$$

With σ fixed, moving one plate outward by an incremental amount dz therefore increases the stored energy by

$$dW = 2\pi\sigma^2 A dz\,, \tag{3.42}$$

leading to the same pressure expression as before.

However, the assumption that σ is constant is not always satisfied. Suppose for example that the plates remain connected to the battery that charged them in the first

place. Then *V*, not σ, is constant. Now to assess force, we must revise Eq. (3.41) to include this new condition. In terms of *V*,

$$W = 2\pi \frac{V^2}{16\pi^2 d^2} Ad = \frac{V^2 A}{8\pi d}. \tag{3.43}$$

Increasing d by a small amount dz now leads to a very different result:

$$dW = -\frac{V^2 A}{8\pi d^2} dz. \tag{3.44}$$

Thus the energy stored in the capacitor has *decreased*. With some thought this is not surprising because with *V* constant, *E* must decrease. Thus *the capacitor has done work moving the plates apart*, which means that if the energy stored in the capacitor were the only consideration, then the plates are now being *pushed* apart with a pressure which by Eq. (3.44) is the negative of that given by Eq. (3.43).

But this cannot be the entire story, since empirical evidence shows that capacitors do not explode when connected to batteries, no matter how poorly the capacitors may be constructed. The answer lies in the fact that we haven't considered the entire picture. σ decreases as the field decreases, so the increase dz in *d* also results in a charge dQ being delivered to the battery. The energy associated with this transfer is obviously VdQ.

Thus to obtain the complete picture, we must calculate dQ. This follows from the relation

$$Q = \sigma A = \frac{AE}{4\pi} = \frac{AV}{4\pi d}. \tag{3.45}$$

Hence

$$dQ = -\frac{AV}{4\pi d^2} dz, \tag{3.46}$$

which requires an expenditure of energy

$$dW' = V\,dQ = \frac{AV^2}{4\pi d^2} dz. \tag{3.47}$$

This is exactly twice as large as the energy given up by the capacitor, so the net effect is the same. There is no free lunch: the conductor is still pulled into the field region, although the mechanism now is entirely different. The take-home message here is that it is important to determine what is being held constant in calculating forces according to energy-conservation principles.

A practical example of mechanical force delivering energy to an electrostatic system occurred the telephone-company environment when information was carried on wires instead of optical fibers. Technicians who worked on (grounded) overhead cable trays were receiving shocks as they touched the trays. Someone finally realized that this was a result of their rubber-soled shoes picking up charge when they walked across floors. This resulted in an electric field $E = 4\pi\sigma$ between the floor and the soles of the shoes. As the technician went up the ladder, this field resulted in a voltage $V = Ed = 4\pi\sigma d$, where *d* is an effective distance between the floor and the shoes. Consequently, the higher the technician climbed the (insulating) ladder, the higher the voltage developed. On reaching the cable tray, the voltage had become high enough to give the technician a good shock. Once the physics was understood, shoe soles were made of conducting material and the problem disappeared.

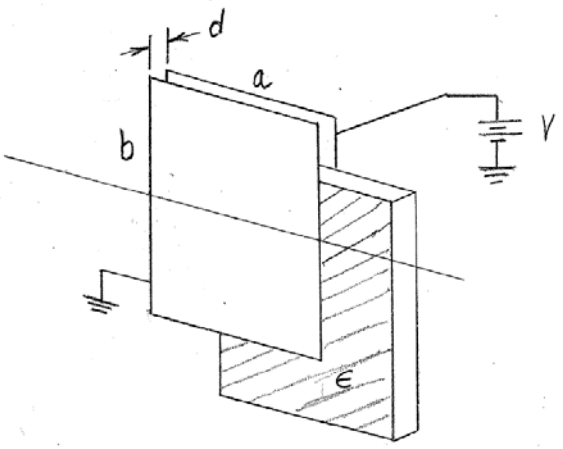

I. Forces on conductors: direct calculations.

Clearly energy considerations are not the only way to determine forces on conductors. They may not even be the best way. Consider for example the direct use of Coulomb's force law in establishing the force on the plates of the capacitor of the previous section. Define a coordinate system where $\Delta q_1 = -\sigma\Delta A$ is the element of charge at the origin on the $z = 0$ plate, and let $\Delta q_2 = \sigma\rho d\rho d\varphi$ be an element at $\vec{r} = \rho\hat{\rho} + \hat{z}d$ on the $z = d$ plate, as shown in the diagram above. Then by Coulomb's force law, we can obtain the force on Δq_1 by evaluating the integral

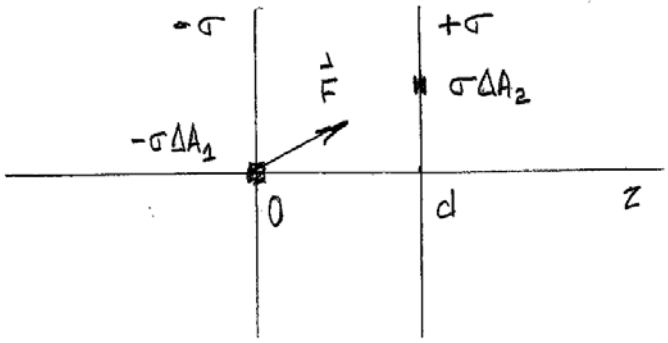

$$\Delta\vec{F} = \int_0^\infty \sigma\rho' d\rho' \int_0^{2\pi} d\varphi' \frac{(-\sigma\Delta A)(\vec{0} - \hat{z}d - \hat{x}\rho'\cos\varphi' - \hat{y}\rho'\sin\varphi')}{|d^2 + \rho'^2|^{3/2}}$$

$$= (2\pi\sigma)(\sigma\Delta A_1)\hat{z}\,. \qquad (3.48)$$

The pressure is then

$$\frac{\Delta\vec{F}}{\Delta A_1} = 2\pi\sigma^2\hat{z}\,, \tag{3.49}$$

which is the same result as before. Not that there was any doubt, but this shows that the energy calculation is correct.

A final way of calculating the force on the lower plate is to use the Lorentz force law $\vec{F} = q\vec{E}$. This provides an excellent example of the microscopic view of configurations, a perspective that we have already introduced, and one that we will use at numerous times during the course. If we proceed without thinking and repeat the calculation for the differential charge $dQ = \sigma dA$ substituting the field between the plates, we obtain

$$\begin{aligned} d\vec{F} &= \vec{E}\,dQ = \sigma dA(4\pi\sigma) \\ &= 4\pi\sigma dA\,. \end{aligned} \tag{3.50}$$

This is large by a factor of 2 relative to all previous calculations, so there is a problem in our approach. That one might arise is suggested because the field on the other side of the sheet is zero, and the decision of which one to use, if either appears to be arbitrary.

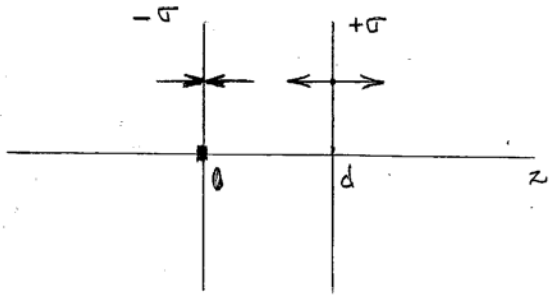

This apparent dilemma is resolved by considering the situation from the perspective of charge placed in empty space. Suppose that the only charge present is the surface charge density $+\sigma$ on the plate at $z = d$ is the only one present. Then by $\nabla\cdot\vec{E} = 4\pi\rho$, Gauss' Theorem, and symmetry, fields of magnitude $E = 2\pi\sigma$ each will point away from the plate on either side. Similarly, the plate with surface charge density $-\sigma$ will generate fields of the same magnitude but pointing toward the plate on either side. As seen in the diagram, the contributions between the plates add, while those outside the plates cancel. This gives a total field of $4\pi\sigma$ between the plates and zero outside, which is consistent with our previous calculation of the field between the plates.

The problem with the above Lorentz-force calculation is now clear. Because a charge does not interact with its own field, the field to use in the calculation is that of the positively charged plate, which half the total field between plates. The apparent discrepancy is resolved.

It can be noted that the same assumption was used without giving it any thought when we used the Coulomb force law to calculate the force on the $+\sigma$ plate.

J. Green functions in one dimension.

Equations (3.2) provide a direct solution of Poisson's Equation in one dimension, so there is no need to look for alternatives. However, this favorable situation does not apply to two or three dimensions, so other approaches are needed. Since the equations are linear, superposition applies so Green functions provide one alternative. The formal

theory of Green functions in three dimensions is given in Ch. 4, but better insight into the nature of the approach and the characteristics of Green-function solutions are obtained by considering the one-dimensional case first.

We divide the treatment into two parts. The first is to find the generic one-dimensional Green function. This is done in the present section. The next is to use Green's Theorem to construct the function that applies to specific configurations and boundary conditions, which is done in the next section. The result is a configuration-specific expression where boundary conditions can be inserted without generating a new function, and at the same time eliminating the need to include solutions of the homogeneous equation. The "what" (the result) is less interesting than the "why" (path to solution), since the "what" addresses the math whereas the "why" addresses the physics.

The Green-function approach bypasses Gauss' Equation entirely, working directly with Poisson's Equation. Assuming otherwise empty space so $\varepsilon = 1$, in one dimension

$$\frac{d^2\phi}{dz^2} = -4\pi\rho(z). \tag{3.51}$$

Now the equation defining the Green function is

$$\frac{d^2G(z,z')}{dz^2} = \frac{d^2G(z,z')}{dz'^2} = -4\pi\delta(z-z'). \tag{3.52}$$

Hence given $G(z,z')$, the formal solution of Eq. (3.51) is clearly

$$\phi(z) = \int_{-\infty}^{\infty} dz'\,\rho(z')G(z,z') + \phi_o(z), \tag{3.53}$$

where $\phi_o(z)$ is a solution of the homogeneous equation $d^2\phi_o(z)/dz^2 = 0$. That Eq. (3.53) is a solution of Eq. (3.51) can be verified immediately by direct substitution:

$$\frac{d^2\phi(z)}{dz^2} = \frac{d^2}{dz^2}\left(\int_{z_1}^{z_2} dz'\,\rho(z')G(z,z')\right) + 0 = \int_{z_1}^{z_2} dz'\,\rho(z')\frac{d^2}{dz^2}G(z,z') \tag{3.54a,b}$$

$$= -4\pi\int_{-\infty}^{\infty} dz'\,\rho(z')\delta(z-z') = -4\pi\rho(z), \tag{3.54c,d}$$

because in the integral, ρ is a function of z', not z. As with any second-order differential equation, $\phi_o(z)$ is used to satisfy boundary conditions, if necessary.

The goal therefore is to determine $G(z,z')$. We start by realizing that $\delta(z-z')$ is mostly zero. In one dimension the solution of the homogeneous equation is obviously

$$\phi_o(z) = a\,z + b, \tag{3.55}$$

where *a* and *b* are constants. This anticipates a procedure that we use extensively in the next 4 chapters, specifically, we can always construct a Green function from solutions of

the corresponding homogeneous equation. Anticipating nonanalytic behavior at $z = z'$, we write $G(z, z')$ in two parts:

$$G(z, z') = az + b \text{ for } z < z' \tag{3.56a}$$

$$= cz + d \text{ for } z > z'. \tag{3.56b}$$

We write Eqs. (3.56) in terms of *z* rather than z' because at this stage we assume the perspective of the observer rather than the dummy variable of integration.

The delta function is also responsible for two general conditions on the coefficients. First, it is created by a *second* derivative, not a first. Hence $G(z, z')$ must be continuous at $z = z'$. Thus one general condition on the coefficients in Eqs. (3.56) is continuity, or

$$az + b = cz + d. \tag{3.57}$$

Second, Eqs. (3.56) must have a discontinuous first derivative at $z = z'$. The value of the discontinuity can be obtained by integrating them over a small range $\pm\delta z$ centered on *z*:

$$\int_{z-\delta z}^{z+\delta z} dz' \frac{d^2\phi(z')}{dz'^2} = \left.\frac{d\phi}{dz'}\right|_{z-\delta z}^{z+\delta z} = c - a \tag{3.58a}$$

$$= -4\pi \int_{z-\delta z}^{z+\delta z} \delta(z - z') = -4\pi. \tag{3.58b}$$

Thus the second condition is

$$a - c = 4\pi. \tag{3.59}$$

The difference $(a - c)$ in the slopes of the two segments of $G(z, z')$ must therefore equal 4π.

As presently formulated, the solutions ϕ_o of the homogeneous equation must be included to match boundary conditions. We can avoid this complication by building the boundary conditions in directly using Green's Theorem. Describing how this is done is the objective of the next section.

K. Green's First Identity and Green's Theorem in one dimension.

Green's Theorem is a remarkable mathematical relation that is based on the one-dimensional version of Gauss' Theorem,

$$\int_{z_1}^{z_2} dz' \frac{d}{dz'} f(z') = f(z_2) - f(z_1). \tag{3.60}$$

The "volume" is the line segment $z_1 \le z' \le z_2$, and the "surface" consists of the end points z_1 and z_2 (note that *V* is completely enclosed by *S*).

Green's insight was to start with the function

$$f(z') = \phi \frac{\partial G}{\partial z'}. \tag{3.61}$$

At the moment ϕ and G are any scalar functions of z', although at the end they will become the potential and the Green function, respectively. Substituting Eq. (3.61) into Eq. (3.60) yields

$$\int_{z_1}^{z_2} dz' \frac{d}{dz'}\left(\phi \frac{\partial G}{\partial z'}\right) = \int_{z_1}^{z_2} dz' \left(\frac{d\phi}{dz'}\frac{\partial G}{\partial z'} + \phi \frac{\partial^2 G}{\partial z'^2}\right) = \phi \frac{\partial G}{\partial z'}\bigg|_{z_1}^{z_2}. \tag{3.62}$$

This is the one-dimensional version of *Green's First Identity*. Next, repeat the calculation with ϕ and G reversed, obtaining

$$\int_{z_1}^{z_2} dz' \frac{d}{dz'}\left(G \frac{d\phi}{dz'}\right) = \int_{z_1}^{z_2} dz' \left(\frac{\partial G}{\partial z'}\frac{d\phi}{dz'} + G \frac{d^2\phi}{dz'^2}\right) = G \frac{d\phi}{dz'}\bigg|_{z_1}^{z_2}. \tag{3.63}$$

Finally, subtract Eq. (3.63) from Eq. (3.62). This eliminates the product of the first derivatives and yields

$$\int_{z_1}^{z_2} dz' \left(\phi \frac{d^2 G}{dz'^2} + G \frac{d^2\phi}{dz'^2}\right) = \left(\phi \frac{\partial G}{\partial z'} - G \frac{d\phi}{dz'}\right)\bigg|_{z_1}^{z_2}. \tag{3.64}$$

This is the one-dimensional version of *Green's Second Identity*, or *Green's Theorem*.

At this stage we have said nothing about ϕ or *G*, so Eq. (3.64) is only a consistency relation. However, let us now require that

$$\frac{\partial^2 G(z,z')}{\partial z'^2} = -4\pi\delta(z - z'), \tag{3.65}$$

where *z* is the location of the observer. Then the first term on the left side of Eq. (3.64) reduces simply to $-4\pi\phi(z)$, assuming that (a) *z* lies in the "volume of interest", i.e., between z_1 and z_2, and (b) there exists only *one* such singularity in this range. We have therefore managed to express $\phi(z)$ anywhere in the interval as an integral plus boundary conditions instead of the solution of a differential equation. This is a huge step forward, because integrals are much easier to deal with than differential equations, may have analytic solutions, and in any case can be evaluated in principle to any level of approximation.

Let us now require that ϕ is the scalar potential. Then since $d^2\phi/dz^2 = -4\pi\rho(z)$, the second Laplacian in the integral of Eq. (3.64) can also be eliminated, with the result

$$\phi(z) = \int_{z_1}^{z_2} dz' \rho(z') G(z,z') \; - \; \frac{1}{4\pi}\left(\phi \frac{\partial G}{\partial z'} - G \frac{d\phi}{dz}\right)\bigg|_{z_1}^{z_2}. \tag{3.66}$$

The solution $\phi_o(z)$ of the homogeneous equation has therefore been replaced by the values of $\phi(z)$ and its derivative at the endpoints of the interval. In principle these boundary conditions, two potentials and two fields, provide the additional constraints needed to evaluate the remaining coefficients in Eqs. (3.56). In short, we have just solved our first boundary-value problem.

However, the above conclusion is not quite correct. With two constraints already in place, the four additional conditions imposed in Eq. (3.66) obviously overspecify the solution. We can fix this by requiring either G, dG/dz', or a combination to be zero at the endpoints. For example, if

$$G(z, z_1) = G(z, z_2) = 0\,, \tag{3.67}$$

then the fields $d\phi/dz'$ are free to assume any values at the endpoints. The two conditions necessary to achieve this are obviously

$$az_1 + b = 0\,; \tag{3.68a}$$

$$cz_2 + d = 0\,; \tag{3.68b}$$

in which case the result is

$$\phi(z) = \int_{z_1}^{z_2} dz' G(z, z')\rho(z') - \frac{1}{4\pi}\phi(z')\frac{\partial G(z, z')}{\partial z'}\bigg|_{z_1}^{z_2}. \tag{3.69}$$

The fields at the endpoints are determined as part of the solution. It can be appreciated that the coefficients a, b, c, and d obtained by solving Eqs. (3.56) and (3.68) are defined entirely by the configuration. The boundary conditions are inserted in Eq. (3.69) after $G(z, z')$ has been obtained.

The particular form of $G(z, z')$ that vanishes on S is the Dirichlet Green function, which is commonly written as $G_D(z, z')$. In principle 3 other combinations are also possible, although one must be excluded as shown below. The allowed versions are $\phi(z)$ specified at $z = z_1$ and $d\phi/dz$ at $z = z_2$, and the inverse, $d\phi/dz$ specified at $z = z_1$ and ϕ at $z = z_2$. In the first case we set $G(z, z') = 0$ at $z' = z_1$ and $d\phi(z')/dz' = 0$ at $z' = z_2$. The equations replacing (3.68) are therefore

$$az_1 + b = 0\,; \tag{3.70a}$$

$$c = 0\,. \tag{3.70b}$$

In the other case we have

$$a = 0\,; \tag{3.71a}$$

$$cz_2 + d = 0\,. \tag{3.71b}$$

If we attempt to set $d\phi/dz' = 0$ at z_1 and z_2 this would require $a = c = 0$ in direct conflict with Eq. (3.59). It is evident that with mixed boundary conditions the Green function is different from $G_D(z,z')$.

With the boundary conditions included in Eq. (3.69), the homogeneous term in Eq. (3.53) is not needed. However, another question can be asked: for a given set of boundary conditions is the solution (3.69) unique, or should we continue look for others? The answer is provided by the uniqueness theorem, which is obtained by considering the one-dimensional version of Green's First Identity, as follows. Let $\phi_1(z)$ and $\phi_2(z)$ be different solutions of Eq. (3.69) but satisfying the same boundary conditions. Start by constructing the difference $\left(\phi_1(z') - \phi_2(z')\right)$ and build $f(z')$ in Eq. (3.60) using this difference, or

$$f(z') = (\phi_1 - \phi_2)\frac{d}{dz'}(\phi_1 - \phi_2) \tag{3.72}$$

(the arguments z' are understood.) Substituting this result in Green' Theorem yields Green's First Identity in the form

$$\int_{z_1}^{z_2} dz' \frac{d}{dz'}\left((\phi_1 - \phi_2)\frac{d}{dz'}(\phi_1 - \phi_2)\right) = \left((\phi_1 - \phi_2)\frac{d(\phi_1 - \phi_2)}{dz'}\right)_{z_1}^{z_2}$$

$$= \int_{z_1}^{z_2} dz' \left((\phi_1 - \phi_2)\frac{d^2(\phi_1 - \phi_2)}{dz'^2} + \left(\frac{d(\phi_1 - \phi_2)}{dz'}\right)^2\right). \tag{3.73}$$

Because the boundary conditions for ϕ_1 and ϕ_2 are the same, we conclude that

$$\int_{z_1}^{z_2} dz' \left(\frac{d(\phi_1 - \phi_2)}{dz'}\right)^2 = 0. \tag{3.74}$$

Thus ϕ_1 and ϕ_2 can differ at most by a constant. However, since they share the same boundary conditions, the constant must be zero. Thus ϕ is unique. We conclude that the Green-function solution yields a consistent set of equations with no contradictions and no loose ends.

We now consider the Dirichlet solution explicitly for a region extending from z_1 to z_2. After some algebra, we find

$$a = 4\pi\frac{z_2 - z}{z_2 - z_1}; \tag{3.75a}$$

$$b = -4\pi z_1\frac{z_2 - z}{z_2 - z_1}; \tag{3.75b}$$

$$c = -4\pi \frac{z - z_1}{z_2 - z_1}; \tag{3.75c}$$

$$d = 4\pi z_2 \frac{z - z_1}{z_2 - z_1}. \tag{3.75d}$$

We have therefore

$$G_D(z, z') = 4\pi \frac{(z_2 - z')(z - z_1)}{z_2 - z_1} \quad \text{for } z' > z; \tag{3.76a}$$

$$= 4\pi \frac{(z_2 - z)(z' - z_1)}{z_2 - z_1} \quad \text{for } z' < z. \tag{3.76b}$$

Equations (3.76) can be collapsed into a single equation by defining $z_>$ and $z_<$ as the greater and lesser, respectively, of z and z'. The compact version of Eqs. (3.76) is then

$$G_D(z, z') = 4\pi \frac{(z_2 - z_>)(z_< - z_1)}{z_2 - z_1}. \tag{3.77}$$

A schematic of the functional dependence is shown in the diagram at the right. It also follows from Eqs. (3.76) that $G(z, z') = G(z', z)$. However, because the boundary conditions have been incorporated, G is not a function of $(z' - z)$. That this is the correct solution is easily verified by inspection.

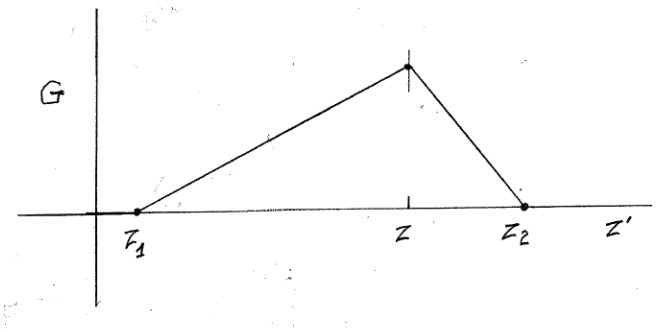

L. Parallel-plate capacitor via Green's Theorem.

As a test, we consider a capacitor consisting of a plate at potential V_1 at $z = z_1$, the second plate at V_2 and $z = z_2$, and $\rho(z) = 0$. Then only the "surface" term in Eq. (3.69) contributes. To evaluate it, we need $\partial G(z, z')/\partial z'$ at $z' = z_1$ and $z' = z_2$. For $z' = z_1$ we have $z \geq z'$, so the appropriate expression to differentiate is Eq. (3.76b). The result is

$$\left.\frac{\partial G(z, z')}{\partial z'}\right|_{z'=z_1} = 4\pi \frac{z_2 - z}{z_2 - z_1}. \tag{3.78}$$

For $z' = z_2$, we have $z \leq z'$, so the expression to differentiate is Eq. (3.68a). The result is

$$\left.\frac{\partial G(z, z')}{\partial z'}\right|_{z'=z_1} = -4\pi \frac{z - z_1}{z_2 - z_1}. \tag{3.79}$$

Putting everything together, Eq. (3.66) becomes)

$$\phi(z) = -\frac{1}{4\pi}V_2\left(-4\pi\frac{z-z_1}{z_2-z_1}\right)+\frac{1}{4\pi}V_1\left(4\pi\frac{z_2-z}{z_2-z_1}\right)$$
$$= \frac{V_1(z_2-z)+V_2(z-z_1)}{(z_2-z_1)} \tag{3.80}$$

The proportionality is exactly what we expect. While the result can be written by inspection, the Green-function result reduces the calculation to crank turning. Crank turning also describes the calculation if $\rho(z) \neq 0$.

Finally, the surface charge densities on the two plates follow from $\hat{n}\cdot\vec{E} = 4\pi\sigma$, where $\hat{n} = \hat{z}$ at $z = z_1$ and $\hat{n} = -z$ at $z = z_2$. With

$$E = -\frac{d\phi}{dz} = -\frac{V_2 - V_1}{z_2 - z_1}, \tag{3.81}$$

we obtain

$$\sigma_1 = -\frac{1}{4\pi}\frac{V_2 - V_1}{z_2 - z_1}; \tag{3.82a}$$

$$\sigma_2 = \frac{1}{4\pi}\frac{V_2 - V_1}{z_2 - z_1}. \tag{3.82b}$$

Again, these are exactly what we expect. Green's Theorem works!

Although our discussion involves only one dimension, the procedure and conclusions are very general and will be used in three-dimensional treatments covered in the next chapter. One takeaway is that Green functions can always be constructed by patching together solutions of the homogeneous equations such that the patch is continuous at the singularity or singularities, but has a discontinuous first derivatives there. Green's Theorem is then used to incorporate boundary conditions and provide additional constraints, leading to a single expression with all terms defined. Constructing these functions is a major objective not only of this chapter but also of the rest of the course.